


Article

Three New Xanthonones from *Hypericum scabrum* and Their Quorum Sensing Inhibitory Activities against *Chromobacterium violaceum*

Li-Ping Teng ^{1,2,†}, Hong Zeng ^{1,†}, Cai-Yan Yang ², He-Bin Wang ^{3,*}  and Zhong-Bo Zhou ^{1,2,*}

¹ Research Center for the Prevention and Treatment of Drug Resistant Microbial Infecting, Youjiang Medical University for Nationalities, Baise 533000, China

² School of Pharmacy, Youjiang Medical University for Nationalities, 98 Chengxiang Road, Baise 533000, China

³ College of Chemical Engineering and Technology, Tianshui Normal University, Tianshui 741000, China

* Correspondence: wanghebin@tsnu.edu.cn (H.-B.W.); zzb7855@163.com (Z.-B.Z.)

† These authors contributed equally to this work.

Abstract: Quorum sensing (QS) plays an important role in the production of virulence factors and pathogenicity in pathogenic bacteria and is, therefore, a hopeful target to fight against bacterial infections. During our search for natural QS inhibitors, two new xanthonolignoids (**1** and **2**), each existing as a racemic mixture, one new simple oxygenated xanthone (**7**), and eight known analogs (**3–6**, **8–11**) were isolated from *Hypericum scabrum* Linn. Chiral separation of **1** yielded a pair of enantiomers **1a** and **1b**. The structures of these compounds were elucidated by spectroscopic analysis and ECD (electrostatic circular dichroism) calculations. All isolates were evaluated for their QS inhibitory activity against *Chromobacterium violaceum*. Both **9** and **10** exhibited the most potent QS inhibitory effects with minimum inhibitory concentration (MIC) and minimum bactericidal concentration (MBC) values of 31.25 and 62.5 μ M, respectively. Crystal violet staining was used to further evaluate the biofilm inhibition potential of compounds **7**, **9** and **10**, and the formation of biofilms increased with decreasing drug concentration in a classic dose-dependent manner. The results of a cytotoxicity assay revealed that compounds **7**, **9** and **10** exhibited no cytotoxic activity on PC-12 cells at the tested concentration.

Keywords: xanthonolignoids; xanthonones; *Hypericum scabrum*; quorum sensing inhibitory activities



Citation: Teng, L.-P.; Zeng, H.; Yang, C.-Y.; Wang, H.-B.; Zhou, Z.-B. Three New Xanthonones from *Hypericum scabrum* and Their Quorum Sensing Inhibitory Activities against *Chromobacterium violaceum*. *Molecules* **2022**, *27*, 5519. <https://doi.org/10.3390/molecules27175519>

Academic Editor: William Setzer

Received: 20 July 2022

Accepted: 25 August 2022

Published: 27 August 2022

Publisher's Note: MDPI stays neutral with regard to jurisdictional claims in published maps and institutional affiliations.



Copyright: © 2022 by the authors. Licensee MDPI, Basel, Switzerland. This article is an open access article distributed under the terms and conditions of the Creative Commons Attribution (CC BY) license (<https://creativecommons.org/licenses/by/4.0/>).

1. Introduction

Microbial infection is still a major public health concern worldwide. Interfering with quorum sensing (QS) systems that regulate the expression of many genes associated with the virulence of pathogens was a promising alternative strategy for controlling bacterial infection, especially for those caused by multi-drug resistant strains [1,2]. *Chromobacterium violaceum* ATCC12472 is one of the most commonly used bacterial species for QS research. Quorum sensing inhibitors (QSIs) are different from conventional antibiotics in that they focus on reducing the virulence of bacteria without killing bacteria or inhibiting bacterial growth. Recently, there has been increasing evidence that phytochemicals can be an important source of QSIs [3,4].

Xanthonones are the main secondary metabolites of plants belonging to the genus *Hypericum*, which is widely distributed in temperate zones of the world and many have been used as folk medicines. Xanthonolignoids are a relatively rare class of natural compounds, most of which have a phenylpropane moiety attached to the xanthone skeleton through a dioxane ring [5,6]. *Hypericum scabrum* is a perennial herb growing mainly in arid rocky hillsides or gravel-sloped lands of Altai in Xinjiang, China and Central Asia, where it is commonly used to treat a variety of disorders of the heart, liver, gallbladder, intestines and bladder [7,8]. In our ongoing research for natural QSIs, eleven xanthonones, including two new xanthonolignoids and one new simple oxygenated xanthone (Figure 1), were

obtained from the whole plants of *H. scabrum*. Herein, we describe the isolation, structure elucidation, and QS inhibitory activities of these compounds against *C. violaceum*.

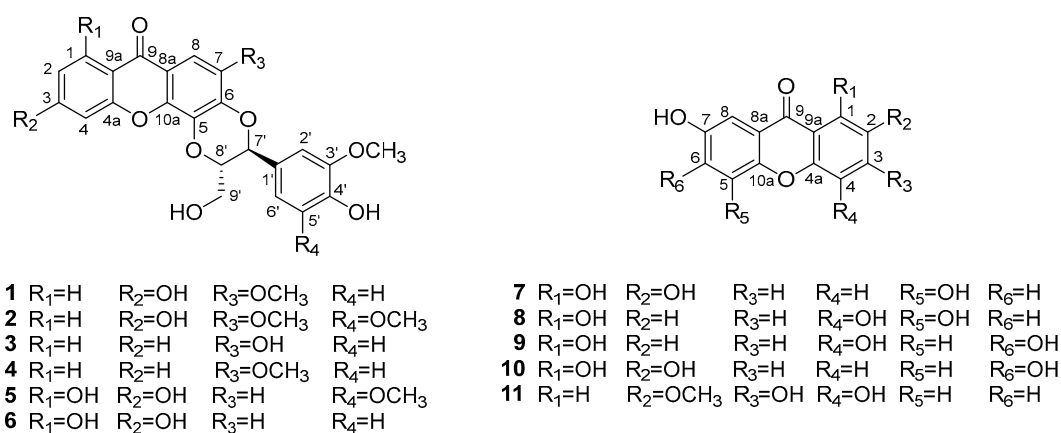


Figure 1. Structures of compounds 1–11.

2. Material and Methods

2.1. General Experimental Procedure

UV spectra were measured on a Shimadzu UV-1800 spectrophotometer. A Thermo Scientific Nicolet iN10 Microscope was used to obtain IR spectra. ECD spectra were measured on a JASCO J1500 CD spectrometer. NMR spectra were acquired in DMSO-*d*₆ at 303 K on a Bruker AVANCE III-500 (¹H NMR, 500 MHz; ¹³C NMR, 125 MHz) with TMS as the internal standard. HRESIMS data were acquired on a Thermo Q-Exactive orbitrap mass spectrometer. Preparative HPLC was performed on a Shimadzu HPLC system consisting of an LC-6AD pump and a Shimadzu SPD-20A detector, coupled with a Shim-park RP-C18 column (5 μm, 200 × 20 mm i.d., Shimadzu, Kyoto, Japan). A Lux Cellulose-2 column (5 μm, 250 × 4.6 mm i.d., Phenomenex, Torrance, CA, USA) was used for chiral separation. Silica gel (200–400 mesh, Qingdao Marine Chemical Co., Ltd.), ODS (40–63 μm, Fuji, Minato, Japan) and Sephadex LH-20 (Pharmacia, Stockholm, Sweden) were used for open column chromatography (CC).

2.2. Plant Material

The whole plants of *Hypericum scabrum* Linn. were collected at Yumin, Xinjiang Uygur Autonomous Region, People's Republic of China, in May 2015 and identified by Dr. Ji-Ye Liang, College of Plant Sciences, Tarim University. A voucher specimen (No. YMUN-201501) was deposited in Research Center for the Prevention and Treatment of Drug Resistant Microbial Infecting, Youjiang Medical University for Nationalities.

2.3. Extraction and Isolation

The air-dried and powdered whole plants of *H. scabrum* (7.9 kg) were extracted with 95% aqueous EtOH (3 × 20 L) under reflux. Removal of the solvent under reduced pressure gave the crude extract (734 g), which was then suspended in H₂O (2 L) and successively partitioned with petroleum ether (3 × 2 L) and ethyl acetate (3 × 2 L). The ethyl acetate extract (179.8 g) was subjected to silica gel CC elution with a gradient of petroleum ether–ethyl acetate (1:0 to 0:1) to give five fractions (A–E). Fraction D (23.8 g) was separated by silica gel CC (petroleum ether–acetone, 5:1, 3:1 and 1:1; ethyl acetate; methanol) to give eight fractions (D1–D8). Fraction D5 (8.0 g) was further separated by LH-20 CC (CHCl₃–MeOH, 1:1) to afford three fractions (D5a–D5c). Fraction D5c (1.1 g) was separated by MPLC using ODS CC (35% MeOH in H₂O) and further purified by preparative HPLC (40% MeOH in H₂O containing 0.1% formic acid, 10 mL/min) to yield **9** (20.4 mg), **10** (6.5 mg) and **11** (5.5 mg). Fraction E (36.8 g) was subjected to silica gel CC eluting with a gradient of methylene dichloride–methanol (20:1 to 0:1) to yield seven fractions (E1–E7). Fraction E2 (3.2 g) was purified by MPLC using ODS CC (MeOH–H₂O,

50:50 to 100:0) to yield three fractions (E2a–E2c). Fraction E2b (439 mg) was purified by HPLC (50% MeOH in H₂O containing 0.1% formic acid, 10 mL/min) to afford **4** (8.6 mg).

Fraction E3 (0.9 g) was separated by ODS MPLC (MeOH–H₂O, 50:50 to 100:0) to yield three fractions (E3a–E3c). Fraction E3a (260 mg) was separated by HPLC (40% MeOH in H₂O containing 0.1% formic acid, 10 mL/min) to afford **7** (6.2 mg) and **8** (2.7 mg). Fraction E3b (619 mg) was separated by HPLC (55% MeOH in H₂O containing 0.1% formic acid, 10 mL/min) to afford six fractions (E3bI–E3bVI). Fraction E3bV (17.6 mg) was purified by preparative HPLC (30% CH₃CN in H₂O containing 0.1% formic acid, 10 mL/min) to give **1** (4.2 mg). Compound **1a** (0.7 mg) and **1b** (0.6 mg) were obtained by using a Lux Cellulose-2 column (88% CH₃CN in H₂O containing 0.1% CH₃COOH, 2 mL/min). Fraction E3bIV (20.8 mg) was purified by preparative HPLC (30% CH₃CN in H₂O containing 0.1% formic acid, 10 mL/min) to yield **2** (1.4 mg) and **3** (1.4 mg). Finally, compounds **5** (2.3 mg) and **6** (2.1 mg) were obtained from Fraction E3bVI (412 mg) by HPLC (30% CH₃CN in H₂O).

6-Hydroxy-kielcorin (**1**): white amorphous powder; ¹³C and ¹H NMR data, see Table 1; HRESIMS *m/z* 451.1043 [M – H][–] (calcd for C₂₄H₁₉O₉, 451.1029).

Table 1. ¹H (500 MHz) and ¹³C NMR (125 MHz) data of compounds **1**, **2**, **7** and **8** (in DMSO-*d*₆).

Position	1		2		7		8	
	δ_{H} (Multiplicity, <i>J</i> in Hz)	δ_{C}	δ_{H} (Multiplicity, <i>J</i> in Hz)	δ_{C}	δ_{H} (Multiplicity, <i>J</i> in Hz)	δ_{C}	δ_{H} (Multiplicity, <i>J</i> in Hz)	δ_{C}
1	8.00 d (8.5)	127.6	7.97 d (8.5)	127.5		147.4		152.3
2	6.86 dd (8.5, 1.5)	114.7	6.84 dd (8.5, 1.5)	114.9		148.2	6.51 d (8.0)	107.8
3		164.9		165.5	7.18 d (8.0)	122.7	7.12 d (8.0)	121.5
4	6.82 ^a	101.9	6.82 ^a	101.9	6.83 d (8.0)	105.4		137.0
4a		157.4		157.5		139.4		143.7
5		132.4		132.4		157.9		158.1
6		138.8		138.7	7.32 s	106.1	7.30 s	105.9
7		145.5		145.4		152.6		152.3
8	7.16 s	96.6	7.16 s	96.6	6.71 s	101.6	6.74 s	101.6
8a		113.9		114.0		109.8		110.1
9		173.7		173.6		180.0		179.5
9a		113.0		112.9		108.0		108.1
10a		141.0		140.9		144.7		145.1
1'		126.7		125.7				
2'	7.05 d (1.5)	112.1	6.77 s	105.7				
3'		147.7		148.0				
4'		147.3		136.2				
5'	6.82 ^a	115.4		148.0				
6'	6.90 dd (8.0, 1.5)	120.8	6.77 s	105.7				
7'	5.05 d (7.5)	76.3	5.04 d (7.5)	76.6				
8'	4.37 m	77.8	4.42 m	77.7				
9'	3.70 dd (12.5, 1.5)	59.9	3.72 d (12.5)	59.9				
	3.42 dd (12.5, 4.0)		3.42 d (12.5)					
7-OCH ₃	3.84 s	55.8	3.85 s	55.7				
3'-OCH ₃	3.78 s	55.7	3.78 s	56.1				
5'-OCH ₃			3.78 s	56.1				

^a overlapped signals.

(+)-6-Hydroxy-kielcorin (**1a**): UV (MeOH) λ_{max} (log ϵ) 244 (4.28), 321 (3.97) nm; $[\alpha]_{\text{D}}^{20} +29.4$ (*c* 0.1, CH₃OH); ECD (*c* = 3.0 × 10^{−4}, MeOH) λ_{max} nm ($\Delta\epsilon$) 379 (+0.28), 342 (+5.5), 302 (−0.91), 293 (+0.66), 289 (+0.55), 280 (+3.6), 269 (+0.44), 253 (+7.5), 235 (−7.3), 219 (+17.3), 202 (−64.4); IR ν_{max} 3386, 2934, 1613, 1572, 1521, 1477, 1439, 1399, 1283, 1259, 1244, 1179, 1136, 1115, 1060, 891, 846, 774 cm^{−1}; HRESIMS *m/z* 475.1003 [M + Na]⁺ (calcd for C₂₄H₂₀O₉Na, 475.1000).

(−)-6-Hydroxy-kielcorin (**1b**): UV (MeOH) λ_{max} (log ϵ) 244 (4.14), 321 (3.82) nm; $[\alpha]_{\text{D}}^{20} -31.2$ (*c* 0.1, CH₃OH); ECD (*c* = 3.0 × 10^{−4}, MeOH) λ_{max} nm ($\Delta\epsilon$) 394 (−0.12), 345 (−6.2), 304 (+0.54), 280 (−4.1), 268 (−1.1), 252 (−7.0), 236 (+5.2), 219 (−16.4), 200 (+49.6); IR ν_{max} 3395, 2925, 1612, 1521, 1476, 1439, 1363, 1284, 1260, 1245, 1180, 1137, 1115, 1060, 1034, 956, 891, 846, 774 cm^{−1}; HRESIMS *m/z* 475.1001 [M + Na]⁺ (calcd for C₂₄H₂₀O₉Na, 475.1000).

6-Hydroxy-3'-methoxy kielcorin (2): white amorphous powder; UV (MeOH) λ_{\max} (log ϵ) 243 (4.11), 320 (3.78) nm; IR ν_{\max} 3356, 2919, 1597, 1427, 1263, 1160, 1112, 1060, 877 cm^{-1} ; ^{13}C and ^1H NMR data, see Table 1; HRESIMS m/z 505.1105 $[\text{M} + \text{Na}]^+$ (calcd for $\text{C}_{25}\text{H}_{22}\text{O}_{10}\text{Na}$, 505.1105).

1,2,5,7-Tetrahydroxyxanthone (7): pale yellow amorphous powder; UV (MeOH) λ_{\max} (log ϵ) 236 (4.30), 293 (3.88), 332 (3.88), 383 (3.93) nm; IR ν_{\max} 3377, 1651, 1612, 1574, 1477, 1288, 1169, 1138, 1051, 801 cm^{-1} ; ^{13}C and ^1H NMR data, see Table 1; HRESIMS m/z 259.0248 $[\text{M} - \text{H}]^-$ (calcd for $\text{C}_{13}\text{H}_7\text{O}_6$, 259.0237).

1,4,5,7-Tetrahydroxyxanthone (8): pale yellow amorphous powder; UV (MeOH) λ_{\max} (log ϵ) 228 (4.07), 255 (4.00), 283 (3.90), 390 (3.71) nm; IR ν_{\max} 3401, 2927, 1612, 1582, 1479, 1281, 1237, 1190, 1154, 1059, 1000, 818 cm^{-1} ; ^{13}C and ^1H NMR data, see Table 1; HRESIMS m/z 259.0248 $[\text{M} - \text{H}]^-$ (calcd for $\text{C}_{13}\text{H}_7\text{O}_6$, 259.0237).

2.4. Anti-QS Assay

C. violaceum ATCC12472 provided by Ocean University of China was used as the target bacterium. The antibacterial activities of isolated compounds (1–11) were screened according to Clinical and Laboratory Standards Institute (CLSI) guidelines. For the QS assay, 100 μL of different concentrations of each compound (0–1 mmol/L) and *C. violaceum* were incubated into a 96-well plate at 30 $^\circ\text{C}$ for 24 h without shaking. Then, the OD₅₉₀ values were measured using a microplate reader (Thermo Fisher), and the minimum inhibitory concentration (MIC) and minimum bactericidal concentration (MBC) values were determined.

To quantify violacein production in *C. violaceum* after treatment with tested compounds, microorganisms in each well were collected and centrifuged for 10 min at 13,000 rpm. After removing the supernatant, an equal volume DMSO was added to precipitates to dissolve the violacein. The solution was then vortexed at maximum velocity for 1 min; the extracted violacein was acquired after another centrifugation (13,000 rpm for 10 min). The absorbance of violacein solution was recorded with a spectrophotometer at 585 nm. The inhibition percentage was calculated based on the formula reported in literature [9].

$$\text{Inhibition rate (\%)} = (\text{OD}_0 - \text{OD}_1) / \text{OD}_0 \times 100\%.$$

OD₀ means OD₅₈₅ of control group. OD₁ represents OD₅₈₅ of treated groups. Each experiment was performed in triplicate by three independent experiments.

To further study their antibacterial activity, inhibition of biofilm formation experiments of compounds 7, 9 and 10 were conducted using a crystal violet assay. Briefly, tested compounds and bacterial suspension were mixed and added into each well of the 96-well microplate. After incubation for 16 h at 37 $^\circ\text{C}$, the medium was removed and washed with sterile water three times. The plates were dried at 65 $^\circ\text{C}$, and 200 μL of 1% (m/v) aqueous solution of crystal violet (CV) was added to stain for 20 min, then thoroughly washed with PBS three times. Subsequently, 100 μL of 95% ethanol was added to each well to dissolve CV at 37 $^\circ\text{C}$ for 30 min. The absorbance at OD 470 nm was then measured to determine the biofilm biomass on a microplate reader [2].

2.5. Cell Viability Assay

PC-12 cells were cultured in DMEM containing 100 mg/mL streptomycin, 100 units/mL penicillin, and 10% (v/v) FBS at 37 $^\circ\text{C}$ and 5% CO₂. PC-12 cell viability was evaluated with 3-(4,5-dimethylthiazole-2-yl)-2,5-diphenyltetrazolium bromide (MTT). Cells were grown in 96-well plates at an initial density of 1×10^4 cells/well for 24 h. Then, the cells were subjected to different concentrations of compounds 7, 9 and 10 (0, 0.97, 1.95, 3.91, and 15.63 μM) for 24 h at 37 $^\circ\text{C}$. Subsequently, the cells were treated with MTT (5 mg/mL in PBS) for 4 h, and a microplate photometer was used for evaluating absorbance at 550 nm.

2.6. ECD Calculations

Conformational analyses were carried out using the MMFF94S force field with an energy cutoff of 2.5 kcal/mol. Subsequently, the low-energy conformers were re-optimized using DFT at the B3LYP/6-311+G(d,p) level in MeOH using the polarizable conductor calculation model (CPCM). The energies, oscillator strengths, and rotational strengths (velocity) of the first 30 electronic excitations were calculated using the TDDFT methodology at the B3LYP/6-311+G(d,p) level in MeOH. The ECD spectra were simulated by the overlapping Gaussian function (half the bandwidth at 1/e peak height, $\sigma = 0.20$ for all) [10]. To get the final spectra, the simulated spectra of the conformers were averaged according to the Boltzmann distribution theory and their relative Gibbs free energy (ΔG).

3. Results and Discussion

Compound **1** was isolated as an amorphous white powder. Its molecular formula was assigned as $C_{24}H_{20}O_9$ on the basis of the HRESIMS (Figure S3) ion peak $[M - H]^-$ at m/z 451.1043 (calcd for $C_{24}H_{19}O_9$, 451.1029). The UV spectrum showed absorption maxima at 244 and 321 nm. The 1H NMR spectrum exhibited signals of several aromatic protons, including a singlet at δ_H 7.16 and those ascribed to two ABX systems [δ 8.00 (1H, d, $J = 8.5$ Hz), 7.05 (1H, d, $J = 1.5$ Hz), 6.90 (1H, dd, $J = 8.0, 1.5$ Hz); 6.86 (1H, dd, $J = 8.5, 1.5$ Hz) and 6.82 (2H, overlapped)]. In addition, signals of two oxygenated methines [δ 5.05, (1H, d, $J = 7.5$ Hz) and 4.37 (1H, m)], two methoxy groups [δ 3.84 (3H, s) and 3.78 (3H, s)], and a hydroxymethyl group [δ 3.70, (1H, dd, $J = 12.5, 1.5$ Hz) and 3.42 (1H, dd, $J = 12.5, 4.0$ Hz)] were observed. These observations suggested that **1** was a xanthonolignoid. Overall, the 1D NMR data of **1** were highly similar to those of known compound kielcorin (**4**) [11,12]. The only difference was that **1** possesses an additional hydroxyl group, which was deduced to be at C-3 based on the HMBC correlations as shown in Figure 2. The HMBC spectrum also showed correlations from H-2' (δ_H 7.05) to C-7', from H-6' (δ_H 6.90) to C-7' and from H-7' (δ_H 5.05) to C-1', confirming that the trisubstituted benzene ring attached at C-7'. Furthermore, HMBC cross-peaks from H-7' (δ_H 5.05) to C-8', from H-8' (δ_H 4.37) to C-7' and from H-9' (δ_H 3.70 and 3.42) to C-8', suggesting that a hydroxymethyl unit linked at C-8'.

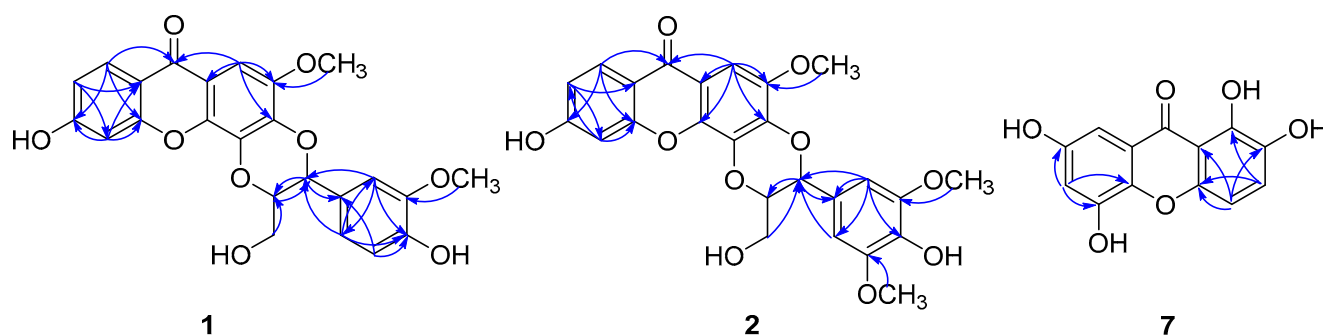


Figure 2. Selected HMBC (arrow) correlations of compounds **1**, **2** and **7**.

Since compound **1** showed no Cotton effect in the ECD spectrum, it was very likely that it was a racemic mixture, which was consistent with the optical rotation value of +0.7. Subsequent chiral resolution of **1** yielded a pair of enantiomers **1a** and **1b** in an approximate ratio of 1:1 (Figure 3), which exhibited mirror image-like ECD curves (Figure 4). The absolute configurations of **1a** and **1b** were defined as (7R, 8R) and (7S, 8S), respectively, by means of ECD calculations.

Compound **2** had a molecular formula of $C_{25}H_{22}O_{10}$ as deduced from its HRESIMS (Figure S8) data (m/z 505.1105 $[M + Na]^+$, calcd for $C_{25}H_{22}O_{10}Na$, 505.1105). The 1H NMR data of **2** revealed typical resonances of a xanthonolignoid, including those of a 1,3,4-trisubstituted aromatic ring [δ 7.97 (1H, d, $J = 8.5$ Hz), 6.84 (1H, dd, $J = 8.5, 1.5$ Hz) and 6.82 (1H, overlapped)], a penta-substituted aromatic ring [δ 7.16 (1H, s)], a tetra-substituted aromatic ring [δ 6.77 (2H, s)], two oxygenated methines [δ 5.04, (1H, d, $J = 7.5$ Hz) and

4.42 (1H, m)], three methoxyl groups [δ 3.85 (3H, s) and 3.78 (6H, s)] and a hydroxymethyl group [δ 3.72, (1H, dd, $J = 12.5, 1.5$ Hz) and 3.45 (1H, dd, $J = 12.5, 4.0$ Hz)]. A comparison of the NMR data of **2** with those of **1** revealed that **2** was the 5'-methoxy derivative of **1**, which was supported by the HMBC data (Figure 2). Accordingly, the structure of **2** was elucidated as 6-hydroxy-5'-methoxy kielcorin. Based on the optical rotation value of +1.1, compound **2** was also considered as a racemic mixture. However, due to the limited amount available, chiral resolution of this compound was not performed.

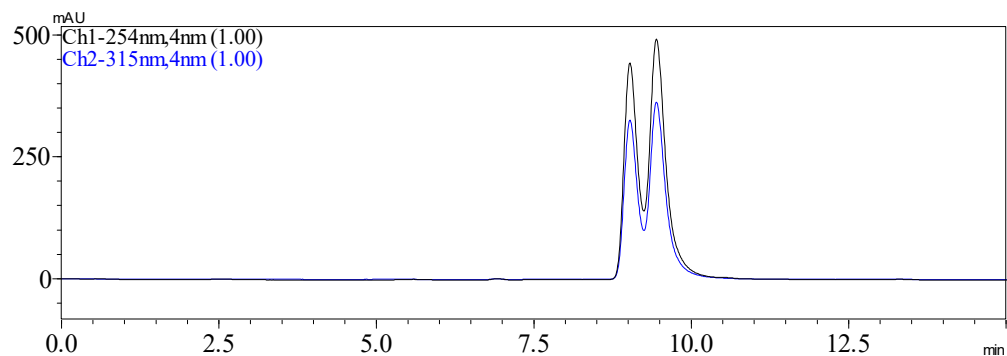


Figure 3. HPLC chromatogram of (±)-6-hydroxy-kielcorin (**1**) on a chiral column.

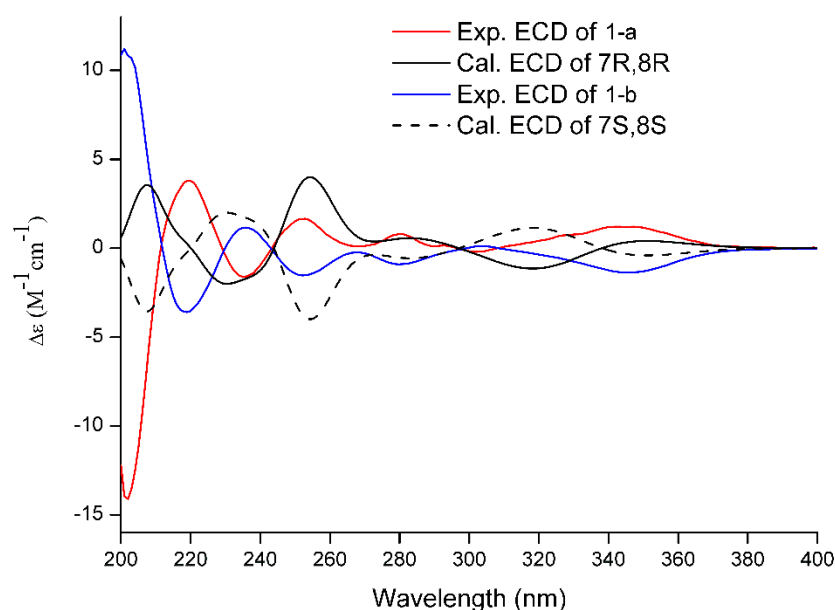


Figure 4. Experimental ECD spectra (200–400 nm) of **1** in MeOH and the calculated ECD spectra of the model molecules of **1** at the B3LYP/6-311+G(d, p) level.

The molecular formula of compound **7**, $C_{13}H_8O_6$, was deduced on the basis of the HRESIMS (Figure S13) ion peak $[M - H]^-$ at m/z 259.0248 (calcd for $C_{13}H_7O_6$, 259.0237). The UV spectrum showed absorptions at 236, 293, 332 and 383 nm, indicating that **7** was a xanthone [12–14]. The 1D NMR data of **7** were comparable to those of 1,2,6,7-tetrahydroxanthone (**9**) [15]. The only difference was that the hydroxyl group at C-6 in **9** was placed at C-5 in **7**, which was confirmed by analysis of HMBC data (Figure 2). Therefore, the structure of **7** was concluded to be 1,2,5,7-tetrahydroxanthone.

In addition to **4** and **9**, the other known compounds were identified as 2-demethylkielcorin (**3**), cadensin G (**5**), 5'-demthoxycadensin G (**6**) [16], 1,4,5,7-tetrahydroxanthone (**8**), 1,4,6,7-tetrahydroxanthone (**10**) [15] and 3,4-dihydroxy-2-methoxyxanthone (**11**) [17] by comparison of their spectroscopic data with those reported. Notably, the UV, IR and NMR data of **8** are reported for the first time in this work.

The genus *Hypericum* is rich in xanthenes that can be classified into xanthonolignoids, prenylated and simple (hydroxy and/or methoxy) xanthenes [16], which were reported to possess various bioactivities [18] such as antibacterial activity [19–21], cytotoxicity, etc. Since *H. scabrum* has been proven to have antimicrobial activity and xanthenes are the main chemical constituents of this plant [22,23], the antibacterial activities of all isolated compounds (1–11) against *C. violaceum* ATCC12472 were screened. As a result (Table 2), compounds 7, 9, 10 and 11 manifested antibacterial activity with MIC ranging from 31.25 to 500 μ M. Notably, all the tested compounds did not inhibit the growth of *C. violaceum* at subinhibitory concentrations of MIC. Based on the results of this study, it appeared that the antibacterial activity of simple xanthenes was stronger than that of xanthonolignoids. The presence of the phenylpropane moiety may decrease the antibacterial activity. In simple xanthenes, 6-OH is essential for the maintenance of antimicrobial effects.

Table 2. The MIC and MBC values of 11 compounds from *Hypericum scabrum* against *C. violaceum* ATCC 12472.

Compounds	MIC (μ M)	MBC (μ M)	MBC/MIC Ratio
1a	>1000	>1000	–
1b	>1000	>1000	–
2	>1000	>1000	–
3	>1000	>1000	–
4	>1000	>1000	–
5	>1000	>1000	–
6	>1000	>1000	–
7	250	500	2
8	>1000	>1000	–
9	31.25	62.5	2
10	31.25	62.5	2
11	125	250	2
kanamycin	13.73	27.46	2

Purple pigment formation is one of the main forms of cell-cell communication used by *C. violaceum* to coordinate their group behavior in response to population density. Compounds 7, 9, 10 and 11 were further assessed for if they can inhibit the purple pigment formation of *C. violaceum*. As shown in Figure 5, at the concentration of 16.53 μ M, these compounds could reduce the formation of purple pigment with an inhibition rate of 21.27%, 75.36%, 76.21% and 53.11%, respectively.

Recent reports suggest that the formation of rigid biofilms on natural and artificial surfaces drastically promotes the resistance capabilities of bacteria. The combination of antibiotics with bacterial biofilm-preventing or disturbing agents seems to be a promising strategy to prevent bacterial infection [24]. The formation of bacterial biofilms is regulated by the QS system. In this study, the biofilm inhibition potential of compounds 7, 9 and 10 was evaluated at different concentrations using crystal violet staining. As shown in Figure 6, the formation of biofilms increased with decreasing drug concentration in a classic dose-dependent manner. At a concentration of 15.63 μ M, the biofilm inhibition rates of compounds 7, 9 and 10 were 55.17%, 86.23% and 74.25%, respectively. These results suggest that compounds 7, 9 and 10 have potential abilities to inhibit the formation of biofilms, which is considered a potential drug target for controlling drug-resistant chronic infections [25].

In light of several studies revealing the cytotoxic activity of xanthenes, the cytotoxic effects of compounds 7, 9 and 10 toward PC-12 cells were evaluated using an MTT assay. As summarized in Figure 7, the three compounds exhibited no cytotoxic activity on PC-12 cells at the concentration of 0.97–15.63 μ M. It's worth noting that compounds 7, 9 and 10 showed more than 50% bacterial biofilm reduction at the concentration of 15.63 μ M but were still safe for PC-12 cells. They showed no obvious damage to PC-12 cells even at the concentrations of MIC and MBC.

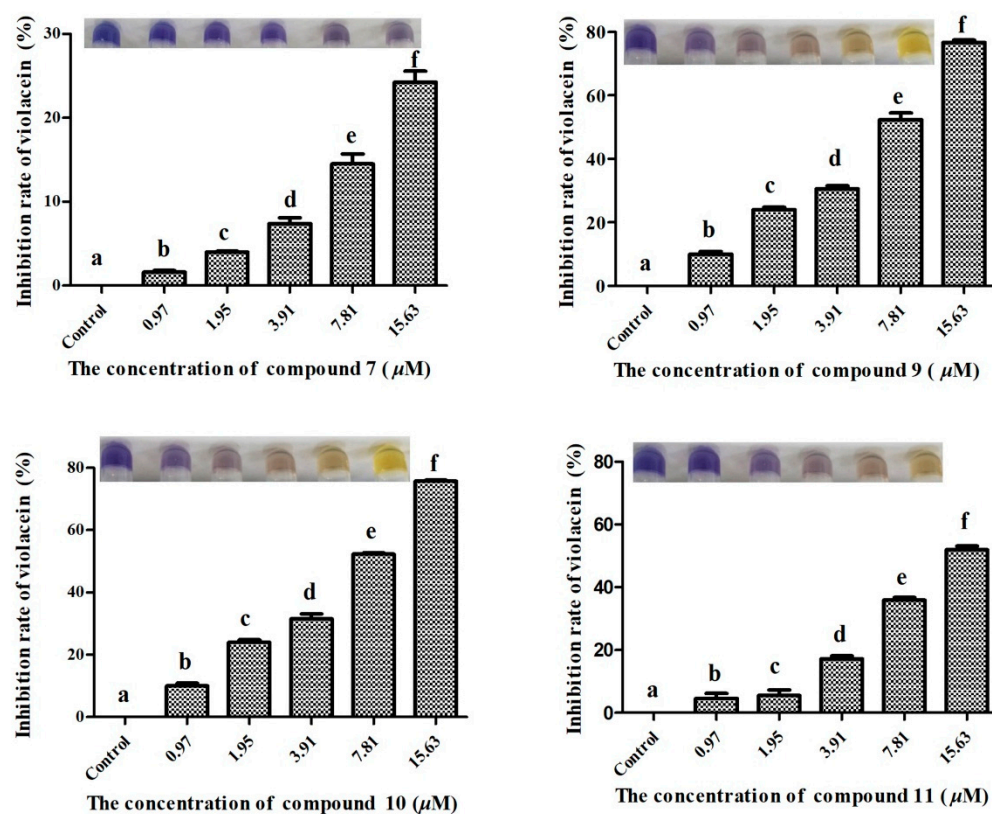


Figure 5. Inhibitory effects of compounds 7, 9, 10 and 11 on purple pigment formation of *C. violaceum* ATCC 12472. Note: The images shown are presented as the means \pm standard deviation from three independent experiments in triplicates. The same letter indicates that the difference is not significant, and the different letters indicate significant differences.

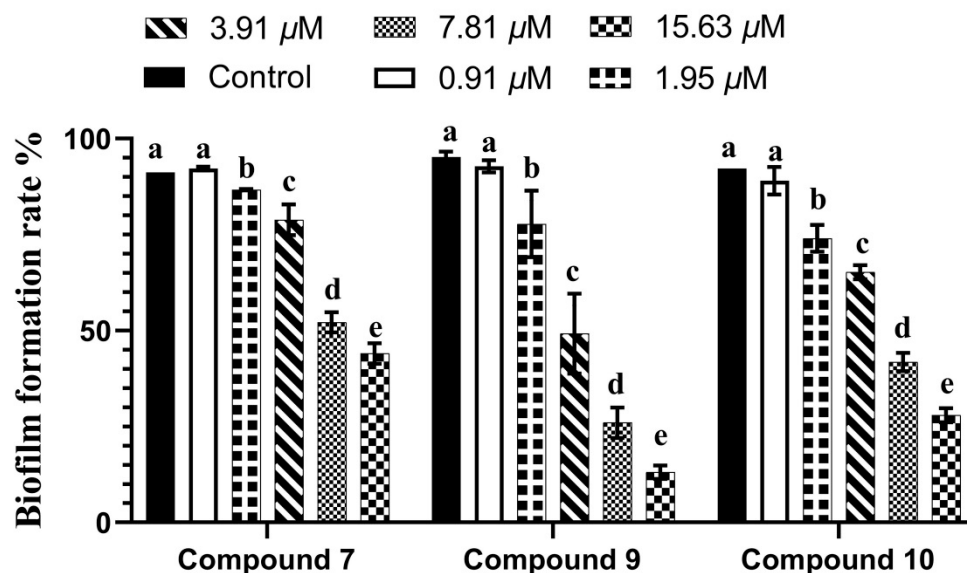


Figure 6. Inhibitory rate of compounds 7, 9 and 10 on *C. violaceum* biofilm formation. Note: Biofilm formation of *C. violaceum* was quantified at OD 490 nm in presence of compounds at 0–15.63 μM 30 °C after 24 h in 96-well plates. Columns represent means \pm standard deviations. Bars with different letters (a–e) differ significantly ($p < 0.05$).

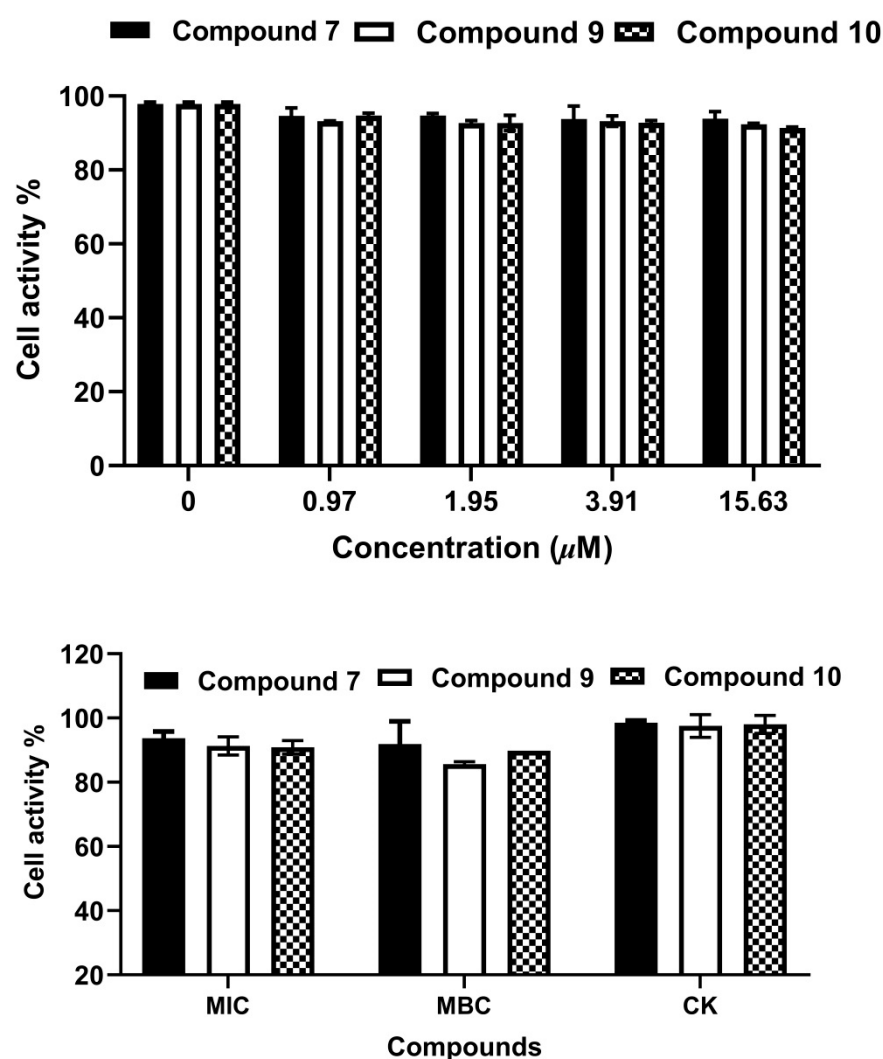


Figure 7. Cytotoxicity of compounds 7, 9 and 10 on PC-12.

QS is a cell-density-dependent communication process to measure population density and trigger appropriate responses and conduct behavioral regulation [26]. QS inhibitors inhibit the QS system by reducing its virulence factor production and biofilm formation without affecting bacterial growth, thus making it difficult to cause drug resistance [27]. The above results signified that bacterial killing was not responsible for the reduction of biofilm formation, and compounds 7, 9 and 10 acted as quorum sensing inhibitors rather than antimicrobial agents. These compounds inhibit QS of *C. violaceum* at sub-inhibitory concentrations representing their unique mechanism for anti-quorum sensing other than growth inhibition or cell death, which was congruent with previous findings [9,28]. Purple pigment and biofilm inhibition potential demonstrated that they act by disturbing the bacterial communication system and attenuating microbial pathogenicity without killing the pathogens. Owing to the insufficient amounts, further anti-quorum sensing mechanism of these compounds was not investigated.

4. Conclusions

As part of our ongoing investigation on natural QSIs, two new xanthonolignoids (1 and 2) each existing as a racemic mixture, one new simple oxygenated xanthone (7) and eight known analogs (3–6, 8–11) were obtained from *H. scabrum*. Chiral separation of 1 yielded a pair of enantiomers 1a and 1b. The structures of these compounds were elucidated by spectroscopic analysis and ECD calculations. The evaluation for the QS inhibitory activity against *C. violaceum* indicated that both 9 and 10 exhibited the most potent QS

inhibitory effects with the minimum inhibitory concentration (MIC) and minimum bactericidal concentration (MBC) values of 31.25 and 62.5 μM , respectively. The antibacterial activity of simple xanthenes was stronger than that of xanthonolignoids. The presence of the phenylpropane moiety may decrease its antibacterial activity, and 6-OH in simple xanthenes is essential for the maintenance of antimicrobial effect, which can be deduced from the analysis of structure–activity relationship. Crystal violet staining was employed to determine the biofilm inhibition potential of compounds **7**, **9** and **10**. The results indicated that the formation of biofilms increased with decreasing drug concentration in a classic dose-dependent manner. The biofilm inhibition rates of these three compounds (15.63 μM) were 55.17%, 86.23% and 74.25%, respectively. The cytotoxic assay results suggested that the three compounds exhibited no cytotoxic activity on PC-12 cells at the concentration of 0.97–15.63 μM , MIC and MBC, which suggested that compounds **7**, **9** and **10** acted as quorum sensing inhibitors rather than antimicrobial agents. They act by inhibiting the formation of purple pigment and biofilm so as to disturb bacterial communication systems and attenuate microbial pathogenicity without killing the pathogens. These findings highlight the importance of the genus *Hepricum* as a source of QS inhibitory compounds.

Supplementary Materials: The following supporting information can be downloaded at <https://www.mdpi.com/article/10.3390/molecules27175519/s1>, Figure S1: ^1H NMR (500 MHz, $\text{DMSO-}d_6$) spectrum of compound **1**; Figure S2: ^{13}C NMR (125 MHz, $\text{DMSO-}d_6$) spectrum of compound **1**; Figure S3: HRESIMS spectrum of compound **1**; Figure S4: HSQC spectrum of compound **1**; Figure S5: HMBC spectrum of compound **1**; Figure S6: ^1H NMR (500 MHz, $\text{DMSO-}d_6$) spectrum of compound **2**; Figure S7: ^{13}C NMR (125 MHz, $\text{DMSO-}d_6$) spectrum of compound **2**; Figure S8: HRESIMS spectrum of compound **2**; Figure S9: HSQC spectrum of compound **2**; Figure S10: HMBC spectrum of compound **2**; Figure S11: ^1H NMR (500 MHz, $\text{DMSO-}d_6$) spectrum of compound **7**; Figure S12: ^{13}C NMR (125 MHz, $\text{DMSO-}d_6$) spectrum of compound **7**; Figure S13: HRESIMS spectrum of compound **7**; Figure S14: HSQC spectrum of compound **7**; Figure S15: HMBC spectrum of compound **7**; Figure S16: ^1H NMR (500 MHz, $\text{DMSO-}d_6$) spectrum of compound **8**; Figure S17: ^{13}C NMR (125 MHz, $\text{DMSO-}d_6$) spectrum of compound **8**; Figure S18: HRESIMS spectrum of compound **8**; Figure S19: HSQC spectrum of compound **8**; Figure S20: HMBC spectrum of compound **8**.

Author Contributions: Conceptualization, Z.-B.Z.; methodology, Z.-B.Z., L.-P.T. and H.Z.; formal analysis, L.-P.T. and C.-Y.Y.; investigation, Z.-B.Z., L.-P.T., and H.Z.; data curation, Z.-B.Z. and H.Z.; writing—original draft preparation, Z.-B.Z. and H.Z.; writing—review and editing, L.-P.T. and C.-Y.Y.; supervision, L.-P.T. and C.-Y.Y.; project administration, Z.-B.Z., H.-B.W. and L.-P.T.; funding acquisition, Z.-B.Z., H.-B.W. and L.-P.T. All authors have read and agreed to the published version of the manuscript.

Funding: This work was supported by National Natural Science Foundation of China, [grant no. 51863018], Guangxi Natural Science Foundation [grant no. 2021GXNSFAA196026, 2020GXNSFAA297063], and the Scientific Research Project for High-Level Talents of Youjiang Medical University for Nationalities [grant no. yy2020bsky044].

Institutional Review Board Statement: Not applicable.

Informed Consent Statement: Not applicable.

Data Availability Statement: Not applicable.

Conflicts of Interest: The authors declare no conflict of interest.

Sample Availability: Samples of the compounds are not available from the authors.

References

1. Sheng, J.Y.; Chen, T.T.; Tan, X.J.; Chen, T.; Jia, A.Q. The quorum-sensing inhibiting effects of stilbenoids and their potential structure-activity relationship. *Bioorg. Med. Chem. Lett.* **2015**, *25*, 5217–5220. [[CrossRef](#)] [[PubMed](#)]
2. Al-Yousef, H.M.; Ahmed, A.F.; Al-Shabib, N.A.; Laeeq, S.; Khan, R.A.; Rehman, M.T.; Alsalmeh, A.; Al-Ajmi, M.F.; Khan, M.S.; Husain, F.M. Onion peel ethylacetate fraction and its derived constituent quercetin 4'-O- β -D glucopyranoside attenuates quorum sensing regulated virulence and biofilm formation. *Front. Microbiol.* **2017**, *8*, 1675–1685. [[CrossRef](#)] [[PubMed](#)]

3. Pejin, B.; Ciric, A.; Glamoclija, J.; Nikolic, M.; Sokovic, M. In vitro anti-quorum sensing activity of phytol. *Nat. Prod. Res.* **2015**, *29*, 374–377. [[CrossRef](#)] [[PubMed](#)]
4. Pejin, B.; Ciric, A.; Karaman, I.; Horvatovic, M.; Glamoclija, J.; Nikolic, M.; Sokovic, M. In vitro antibiofilm activity of the freshwater bryozoan *Hyalinella punctate*: A case study of *Pseudomonas aeruginosa* PAO1. *Nat. Prod. Res.* **2016**, *30*, 1847–1850. [[CrossRef](#)]
5. Pinto, M.M.M.; Sousa, E.P. Natural and synthetic xanthonolignoids: Chemistry and biological activities. *Curr. Med. Chem.* **2003**, *10*, 1–12. [[CrossRef](#)]
6. Mandal, S.; Das, P.C.; Joshi, P.C. Naturally occurring xanthenes from terrestrial flora. *J. Indian Chem. Soc.* **1992**, *69*, 611–636.
7. Li, Y.H.; Wu, Z.Y. (Eds.) *Flora of China*; Science Press: Beijing, China, 1990; p. 50.
8. Liu, R.; Su, Y.; Yang, J.; Wang, A. Polyprenylated acylphloroglucinols from *Hypericum scabrum*. *Phytochemistry* **2017**, *142*, 38–50. [[CrossRef](#)]
9. Mu, Y.; Zeng, H.; Chen, W. Okanin in *Coreopsis tinctoria* Nutt is a major quorum-sensing inhibitor against *Chromobacterium violaceum*. *J. Ethnopharmacol.* **2020**, *260*, 113017. [[CrossRef](#)]
10. Stephens, P.J.; Harada, N. ECD cotton effect approximated by the Gaussian curve and other methods. *Chirality* **2010**, *22*, 229–233. [[CrossRef](#)]
11. Abou-Shoer, M.; Habib, A.A.; Chang, C.J.; Cassady, J.M. Seven xanthonolignoids from *Psorospermum febrifugum*. *Phytochemistry* **1989**, *28*, 2483–2487. [[CrossRef](#)]
12. Wu, Q.L.; Wang, S.P.; Du, L.J.; Yang, J.S.; Xiao, P.G. Xanthenes from *Hypericum japonicum* and *H. Henryi*. *Phytochemistry* **1998**, *49*, 1395–1402. [[CrossRef](#)]
13. Ali, M.; Arfan, M.; Ahmad, M.; Singh, K.; Anis, I.; Ahmad, H.; Choudhary, M.I.; Shah, M.R. Anti-inflammatory xanthenes from the twigs of *Hypericum oblongifolium* Wall. *Planta Med.* **2011**, *77*, 2013–2018. [[CrossRef](#)] [[PubMed](#)]
14. Cardona, M.L.; Fernández, M.I.; Pedro, J.R.; Seoane, E.; Vidal, R. Additional new xanthenes and xanthonolignoids from *Hypericum canariensis*. *J. Nat. Prod.* **1986**, *49*, 95–100. [[CrossRef](#)]
15. Lorenz, P.; Heller, A.; Bunse, M.; Heinrich, M.; Berger, M.; Conrad, J.; Stintzing, F.C.; Kammerer, D.R. Structure elucidation of the main tetrahydroxanthenes of *Hypericum* seeds and investigations into the testa structure. *Chem. Biodivers.* **2018**, *15*, e1800035. [[CrossRef](#)]
16. Tanaka, N.; Kashiwada, Y.; Kim, S.Y.; Sekiya, M.; Ikeshiro, Y.; Takaishi, Y. Xanthenes from *Hypericum chinense* and their cytotoxicity evaluation. *Phytochemistry* **2009**, *70*, 1456–1461. [[CrossRef](#)] [[PubMed](#)]
17. Ali, M.; Latif, A.; Zaman, K.; Arfan, M.; Maitland, D.; Ahmad, H.; Ahmad, M. Anti-ulcer xanthenes from the roots of *Hypericum oblongifolium* Wall. *Fitoterapia* **2014**, *95*, 258–265. [[CrossRef](#)] [[PubMed](#)]
18. Pinto, M.M.M.; Sousa, M.E.; Nascimento, M.S.J. Xanthone derivatives: New insights in biological activities. *Curr. Med. Chem.* **2005**, *12*, 2517–2538. [[CrossRef](#)]
19. Sriyatep, T.; Siridechakorn, I.; Maneerat, W.; Pansanit, A.; Ritthiwigrom, T.; Andersen, R.J.; Laphookhieo, S. Bioactive prenylated xanthenes from the young fruits and flowers of *Garcinia cowa*. *J. Nat. Prod.* **2015**, *78*, 265–271. [[CrossRef](#)]
20. Koh, J.J.; Lin, S.; Aung, T.T.; Lim, F.; Zou, H.; Bai, Y.; Li, J.; Lin, H.; Pang, L.M.; Koh, W.L.; et al. Amino acid modified xanthone derivatives: Novel, highly promising membrane-active antimicrobials for multidrug-resistant gram-positive bacterial infections. *J. Med. Chem.* **2015**, *58*, 739–752. [[CrossRef](#)]
21. Nguemaving, J.; Azebaze, A.; Kuete, V.; Eric Carly, N.; Beng, V.; Meyer, M.; Blond, A.; Bodo, B.; Nkengfack, A. Laurentixanthenes A and B, antimicrobial xanthenes from *Vismia laurentii*. *Phytochemistry* **2006**, *67*, 1341–1346. [[CrossRef](#)]
22. Matsuhisa, M.; Shikishima, Y.; Takaishi, Y.; Honda, G.; Ito, M.; Takeda, Y.; Shibata, H.; Higuti, T.; Kodzhimatov, O.K.; Ashurmetov, O. Benzoylphloroglucinol derivatives from *Hypericum scabrum*. *J. Nat. Prod.* **2002**, *65*, 290–294. [[CrossRef](#)]
23. Tanaka, N.; Takaishi, Y.; Shikishima, Y.; Nakanishi, Y.; Bastow, K.; Lee, K.H.; Honda, G.; Ito, M.; Takeda, Y.; Kodzhimatov, O.K.; et al. Prenylated benzophenones and xanthenes from *Hypericum scabrum*. *J. Nat. Prod.* **2004**, *67*, 1870–1875. [[CrossRef](#)] [[PubMed](#)]
24. Sharafutdinov, I.S.; Pavlova, A.S.; Khabibrakhmanova, A.M.; Faizova, R.G.; Kurbanalieva, A.R.; Tanaka, K.; Trizna, E.Y.; Baidamshina, D.R.; Bogachev, M.I.; Kayumov, A.R. Targeting *Bacillus cereus* cells: Increasing efficiency of antimicrobials by the bornylpossessing 2(5H)-furanone derivative. *New Microbiol.* **2019**, *42*, 29–36. [[PubMed](#)]
25. Wu, H.; Moser, C.; Wang, H.Z.; Hoiby, N.; Song, Z.H. Strategies for combating bacterial biofilm infections. *Int. J. Oral Sci.* **2015**, *7*, 1–7. [[CrossRef](#)] [[PubMed](#)]
26. Papenfort, K.; Bassler, B.L. Quorum sensing signal-response systems in gram-negative bacteria. *Nat. Rev. Microbiol.* **2016**, *14*, 576–588. [[CrossRef](#)]
27. Jiang, T.; Li, M. Quorum sensing inhibitors: A patent review. *Expert Opin. Ther. Patents* **2013**, *23*, 867–894. [[CrossRef](#)]
28. Burt, S.A.; Ojo-Fakunle, V.T.A.; Woertman, J.; Veldhuizen, E.J.A. The natural antimicrobial carvacrol inhibits quorum sensing in *Chromobacterium violaceum* and reduces bacterial biofilm formation at sub-lethal concentrations. *PLoS ONE* **2014**, *9*, e93414.